

A PROGRAM TO STUDY  
CH REACTIONS RELEVANT TO  
COMBUSTION/GASIFICATION PROCESSES

Final Report No. DOE-ER/13269-4  
July 1983 - July 1988

Prepared By:

S.M. Anderson, A. Freedman, and C.E. Kolb  
Center for Chemical and Environmental Physics  
Aerodyne Research, Inc.  
45 Manning Road  
Billerica, MA 01821

Prepared For:

Dr. A.H. Laufer  
Division of Chemical Sciences  
Office of Basic Energy Sciences  
U.S. Department of Energy  
Washington, DC 20545

Contract No. DE-FG02-84ER13269

**DISCLAIMER**

This report was prepared as an account of work sponsored by an agency of the United States Government. Neither the United States Government nor any agency thereof, nor any of their employees, makes any warranty, express or implied, or assumes any legal liability or responsibility for the accuracy, completeness, or usefulness of any information, apparatus, product, or process disclosed, or represents that its use would not infringe privately owned rights. Reference herein to any specific commercial product, process, or service by trade name, trademark, manufacturer, or otherwise does not necessarily constitute or imply its endorsement, recommendation, or favoring by the United States Government or any agency thereof. The views and opinions of authors expressed herein do not necessarily state or reflect those of the United States Government or any agency thereof.

January 1989

MASTER

TABLE OF CONTENTS

<u>Section</u>		<u>Page</u>
1.0	INTRODUCTION .....	1-1
2.0	SUMMARY .....	2-1
	2.1 Year 1 .....	2-1
	2.2 Year 2 .....	2-1
	2.3 Year 3 .....	2-2
	2.4 Year 4 .....	2-2
3.0	DISCUSSION OF RECENT RESULTS .....	3-1
	3.1 Radical Source .....	3-1
	3.2 Spectroscopy .....	3-1
	3.3 Kinetic Studies .....	3-6
	3.3.1 Overview .....	3-6
	3.3.2 Procedure .....	3-6
	3.3.3 Results and Discussion .....	3-9
	3.4 Experiments at Elevated Temperatures .....	3-15
	3.5 Product Channel Observations .....	3-16
	3.5.1 Overview .....	3-16
	3.5.2 Procedure .....	3-16
	3.5.3 Results and Discussion .....	3-17
4.0	CONCLUSIONS .....	4-1
5.0	REFERENCES .....	5-1

APPENDIX A

I. FAST FLOW STUDIES OF CH RADICAL KINETICS AT 290 K

II. THE CH + CO REACTION: RATE COEFFICIENT FOR CARBON ATOM EXCHANGE AT 294 K

*Reprints + Preprints Removed*

## LIST OF ILLUSTRATIONS

<u>Figure</u>		<u>Page</u>
1	Schematic Diagram of the Alkali + Haloform CH Radical Source Positioned Within the Main Flow Tube .....	2-3
2	Laser Excitation Spectra for CH (above) and CD (below), the Latter Obtained By Reacting CH with Excess D <sub>2</sub> .....	3-2
3	Laser Excitation Spectra in the 0-0 Band of the CH(A + x) transition near 432 nm .....	3-3
4	Plot of <sup>13</sup> C Isotopic Shifts for CH. The □ represent observations at Aerodyne, Δ is the single MODR measurement, and + are the data of Ref. 17 .....	3-5
5	A Typical Decay (left) for CH + N <sub>2</sub> , Showing Injector Traverses with Ar (Δ), N <sub>2</sub> (•) and the N <sub>2</sub> /Ar Signal Ratios (∇) .....	3-8
6	Comparison of Our Results with Those of Other Laboratories .....	3-10
7	a) Pseudo First-order Decays Observed in the Overall Reaction of <sup>12</sup> CH with <sup>13</sup> CO .....	3-13
8	Traces of OH LIF Signals As a Function of Time, During Reaction of CH with NO (left) and O <sub>2</sub> (right) .....	3-14

LIST OF TABLES

<u>Table</u>		<u>Page</u>
1	Experimentally Determined Shifts for $^{13}\text{CH}(A \leftarrow X)$ Spectral Lines .....	3-4
2	Bimolecular Rate Coefficient for CH Reactions at 2 Torr He Near Room Temperature Measured Using the Aerodyne Fast-flow Reactor .....	3-9

## 1.0 INTRODUCTION

The goal of the proposed work has been to study a small, but important family of CH reactions of interest in combustion-related systems; namely  $\text{CH} + \text{N}_2$ ,  $\text{H}_2$ ,  $\text{O}_2$ ,  $\text{NO}$ , and  $\text{N}_2\text{O}$ . Until now, these reactions have been studied almost exclusively by IR or UV flash photolysis at moderate temperatures, and little quantitative information about product species has been obtained.<sup>1</sup> The explicit objectives of the present effort were: 1) to develop and characterize a new CW source of CH radicals suitable for use in a fast-flow reactor, 2) to use this source to measure rate constants for several key CH reactions as a function of temperature, and 3) to detect the product channels of these reactions wherever possible. A major portion of these goals have been fulfilled to date. Our accomplishments include: the successful development of a chemical source of CH radicals; the measurement of eight rate constants at 300 K (which agree with previously reported values where available); the detection of OH produced by the  $\text{CH} + \text{NO}$  and  $\text{O}_2$  reactions; the completion of a thorough study of isotopic exchange in the products of the reaction  $\text{CH} + \text{CO}$ ; and, finally, the taking of the first steps to extending this work to higher temperatures.

The reactions cited above are important for a variety of reasons which are discussed briefly here. The  $\text{CH} + \text{N}_2$  process is believed to be the precursor of prompt NO in hydrocarbon flames.<sup>2-3</sup> This is probably because CH is the only radical which can break the strong  $\text{N}_2$  bond at flame-front temperatures. Two separate studies, one in a flame<sup>2</sup> and the other at lower temperatures where recombination dominates occurs,<sup>4</sup> have been reported. A single experiment covering the full range is necessary. Our careful study of isotopic exchange in the  $\text{CH} + \text{CO}$  reaction, which is isoelectronic with the  $\text{CH} + \text{N}_2$  reaction, was also undertaken to expand our understanding of the dynamics of the reaction with  $\text{N}_2$ .

Not only is  $\text{CH} + \text{H}_2$  the simplest methylidyne reaction, it is mechanistically interesting at easily accessible temperatures and amenable to comparison with theory.<sup>5-7</sup> It serves as a reliable touchstone for comparing various experimental methods.

All work to date<sup>5,8-9</sup> suggests that the  $\text{CH} + \text{O}_2$  and  $\text{NO}$  reactions are fast, with weak temperatures dependences.<sup>10</sup> Many possible product channels are available; 3 and 5 ground state sets for  $\text{O}_2$  and  $\text{NO}$ , respectively. Electronically excited  $\text{OH}$  has been detected from the  $\text{O}_2$  reaction,<sup>11</sup> and  $\text{NH(A)}$  and  $\text{CO(v)}$  have been observed from the  $\text{NO}$  process.<sup>11-12</sup> Quantitative measurements of branching ratios are needed for models of  $\text{NO}_x$  production in combustion.

Reactions of  $\text{CH}$  with  $\text{N}_2\text{O}$ , an important greenhouse gas which may be produced in large amounts in stationary power plant combustors, are also fast at room temperature.<sup>9</sup> Even so, current models neglect this destruction mechanism.<sup>3</sup> The identity of the product channels of the reaction (either  $\text{N}_2$  or  $\text{NO}$ ) are important, and may play a significant role in nitrogen chemistry of flames.

The new methods developed to study  $\text{CH}$  chemistry have been discussed extensively in the first publication to come out of this effort,<sup>13</sup> and are only briefly summarized in this report. The fast-flow reactor configuration is ideal for studying the kinetics and mechanisms of  $\text{CH}$  radical reactions. The Aerodyne high temperature flow system is particularly well-suited to coherent investigations over a wide temperature range. The results of these studies of key elementary reactions should be of great value to the kinetics and combustion communities.

## 2.0 SUMMARY

### 2.1 Year 1

In the first year of our present program, we investigated a chemical CW source of carbyne radicals suitable for kinetic studies in fast-flow reactors. Our approach uses alkali metal atoms ( $M = \text{Na}$  or  $\text{K}$ ) to successively abstract halogen ( $X = \text{Br}$  or  $\text{Cl}$ ) atoms from a haloform molecule,



producing the CH radical and three alkali halide molecules. For  $M = \text{Na}$ , the  $\text{CH} + M \rightarrow \text{C} + \text{MH}$  reaction is highly endothermic ( $\Delta H = 33$  kcal/mole) and  $M + \text{CH}$  recombination is slow, precluding consumption of CH radicals by M atoms.

Experiments conducted in the Aerodyne high temperature flow reactor succeeded in producing CH, which was identified by LIF spectroscopy of the  $X^2\Pi$  ( $v'' = 0$ )  $\rightarrow$   $A^2\Delta$  ( $v' = 0$ ) transition near 430 nm. Measurements of CH losses on the reactor wall showed them to be large, approaching unit probability per collision, and the number of radicals produced per bromoform molecule was estimated to be about 1/10 by comparison with LIF of nitric oxide.

### 2.2 Year 2

Early in the second year, attempts to observe CH reacting with  $\text{O}_2$ ,  $\text{H}_2$ , and  $\text{N}_2$  produced mixed results. These and other experiments suggested that better separation between CH production and reaction zones was necessary. A pre-reactor assembly that permits variation of nearly all source parameters independent of main reactor conditions was designed and constructed, and has been used in all subsequent work. A diagram of the radical source positioned

in the flow reactor appears in Figure 1. We learned a great deal about the chemistry of the  $M + \text{CHX}_3$  source, found optimum CH production conditions, and performed preliminary experiments yielding rate coefficients for CH reacting with  $\text{Cl}_2$  and  $\text{O}_2$  at 300 K.

### 2.3 Year 3

The third year of the program proved to be more fruitful, yielding high quality kinetic data for five CH reactions ( $\text{CH} + \text{Cl}_2$ ,  $\text{N}_2\text{O}$ ,  $\text{CH}_4$ ,  $\text{O}_2$ , and  $\text{H}_2$ ), and preliminary results for three others ( $\text{D}_2$ ,  $\text{NO}$  and  $\text{N}_2$ ) at 2 Torr and 290 K. This was the first study of the  $\text{CH} + \text{Cl}_2$  reaction. In addition, we made preliminary observations of significant OH production from both the  $\text{CH} + \text{O}_2$  and  $\text{NO}$  reactions. Initial attempts to operate at higher temperatures (up to 1100 K) revealed a needed design change in the source.

### 2.4 Year 4

In the final year of this effort, we began construction of a new source subassembly incorporating the design changes indicated by our experience in Year 3. All the necessary parts have been fabricated, and the unit is ready for assembly. While this was underway, we used the existing radical source to study several reactions near room temperature, including  $\text{CH} + \text{CO} + \text{M}$ , and the CH and CD + HD and  $^{12}\text{CH} + ^{13}\text{CO}$  isotope exchange processes. We concentrated on the CO reaction due to its similarities to the important  $\text{CH} + \text{N}_2$  process, and to  $^1\text{CH}_2 + \text{CO}$ . The  $^{13}\text{C}$  study resulted in a second publication,<sup>14</sup> and what to our knowledge are the first measurements of isotopic line shifts for low J in the  $A \leftarrow X$  transition of CH. This spectroscopic work should be of interest to other investigating the chemistries of CH and  $\text{CH}_2$  and will shortly be published as a separate study.



# CH RADICAL SOURCE

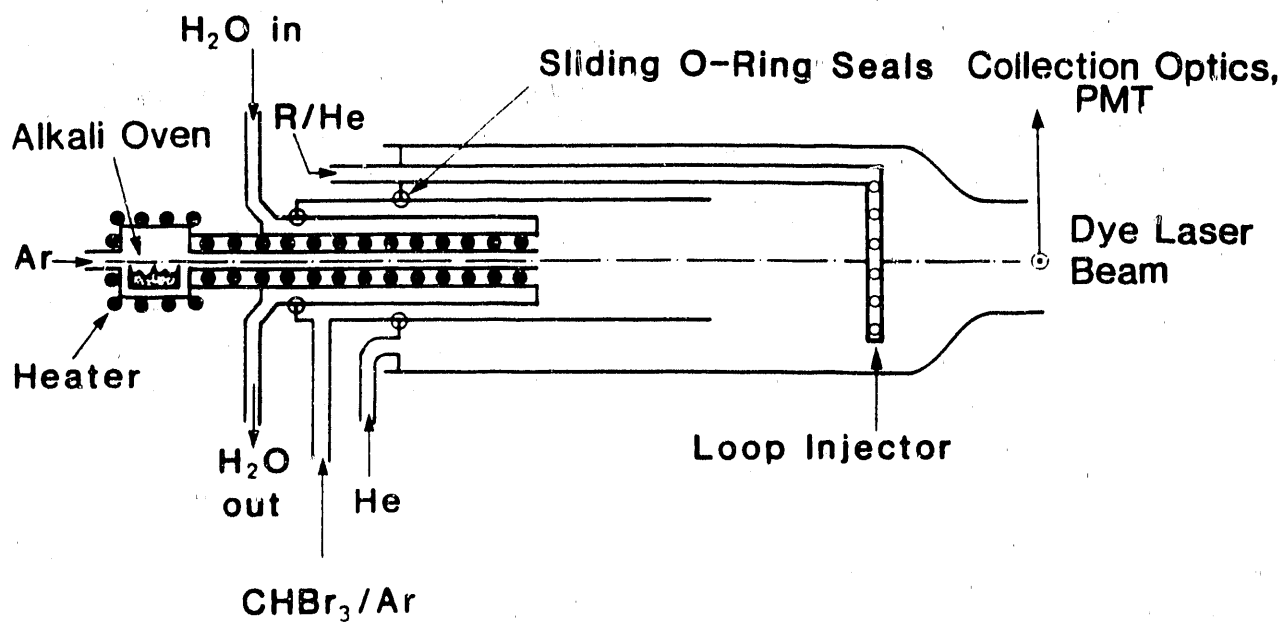
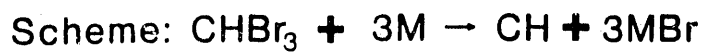


Figure 1. Schematic Diagram of the Alkali + Haloform CH Radical Source Positioned Within the Main Flow Tube //

### 3.0 DISCUSSION OF RECENT RESULTS

#### 3.1 Radical Source

The development and characterization of a simple, CW radical source is the key to successful fast-flow experiments. For CH, this has not been accomplished until now. The components of the source reactor designed and built under this contract are indicated in Figure 1.

Studies conducted to characterize the alkali + haloform system suggested optimum operating parameters for carrying out kinetic and mechanistic investigations. Briefly, the source works well for moderate alkali concentrations ( $5-7 \times 10^{12} \text{ cm}^{-3}$ ), haloform levels below stoichiometric ( $[M]/[\text{CHX}_3] > 10$ ) and contact times slightly longer than required for maximum radical production. The  $\text{CHX}_3 \rightarrow \text{CH}$  conversion efficiency, estimated to be  $\approx 20\%$ , is ample for kinetic measurements. These properties have been independent of the identities of M (Na or K) or X (Br or Cl).

#### 3.2 Spectroscopy

Typical low resolution laser excitation spectra, obtained for CH and CD (produced from the CH + D<sub>2</sub> reaction), are shown in Figure 2. These spectra agree well with those reported previously.<sup>6</sup> For the C-atom exchange experiments, <sup>13</sup>CH-<sup>12</sup>CH spectroscopic line shifts were needed. The only previous systematic study was confined to high J transitions in the R-branch that were too weak to be useful. We therefore examined the strongest low J transitions, P(3) - P(7) and R(1) through R(4), using an intracavity etalon to narrow the dye laser linewidth. Line shifts were determined with an accuracy of  $\pm 0.03 \text{ cm}^{-1}$  from pressure-tuned excitation spectra for mixtures of <sup>12</sup>CH and <sup>13</sup>CH and identical scans for nearly pure <sup>12</sup>CH; Figure 3 shows samples for the P(3) multiplet. The wavelength scale was verified by comparison between our

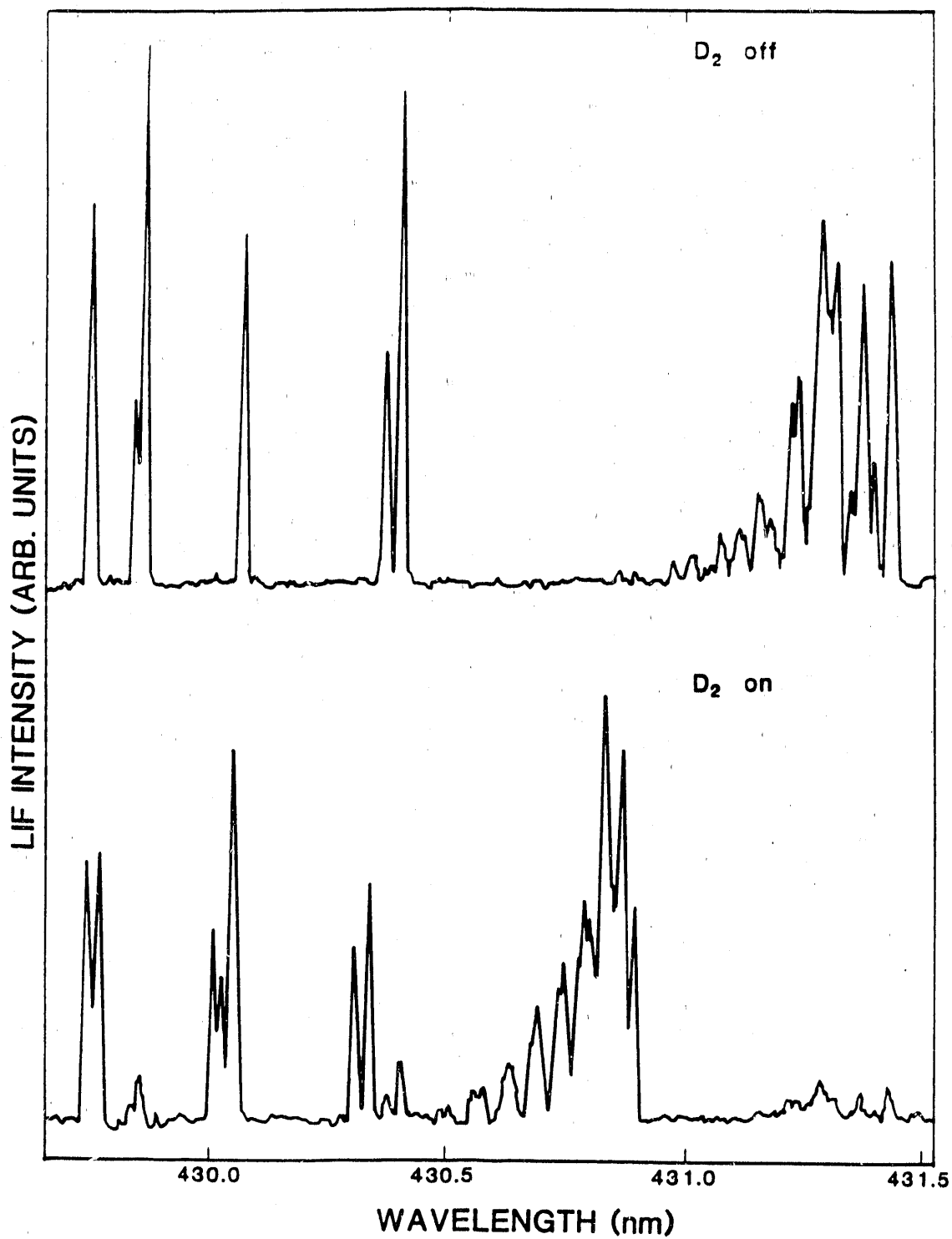


Figure 2. Laser Excitation Spectra for CH (above) and CD (below), the latter obtained by reacting CH with excess D<sub>2</sub>. A small amount of CH ( $\approx 10\%$ ) is present in the CD scan.

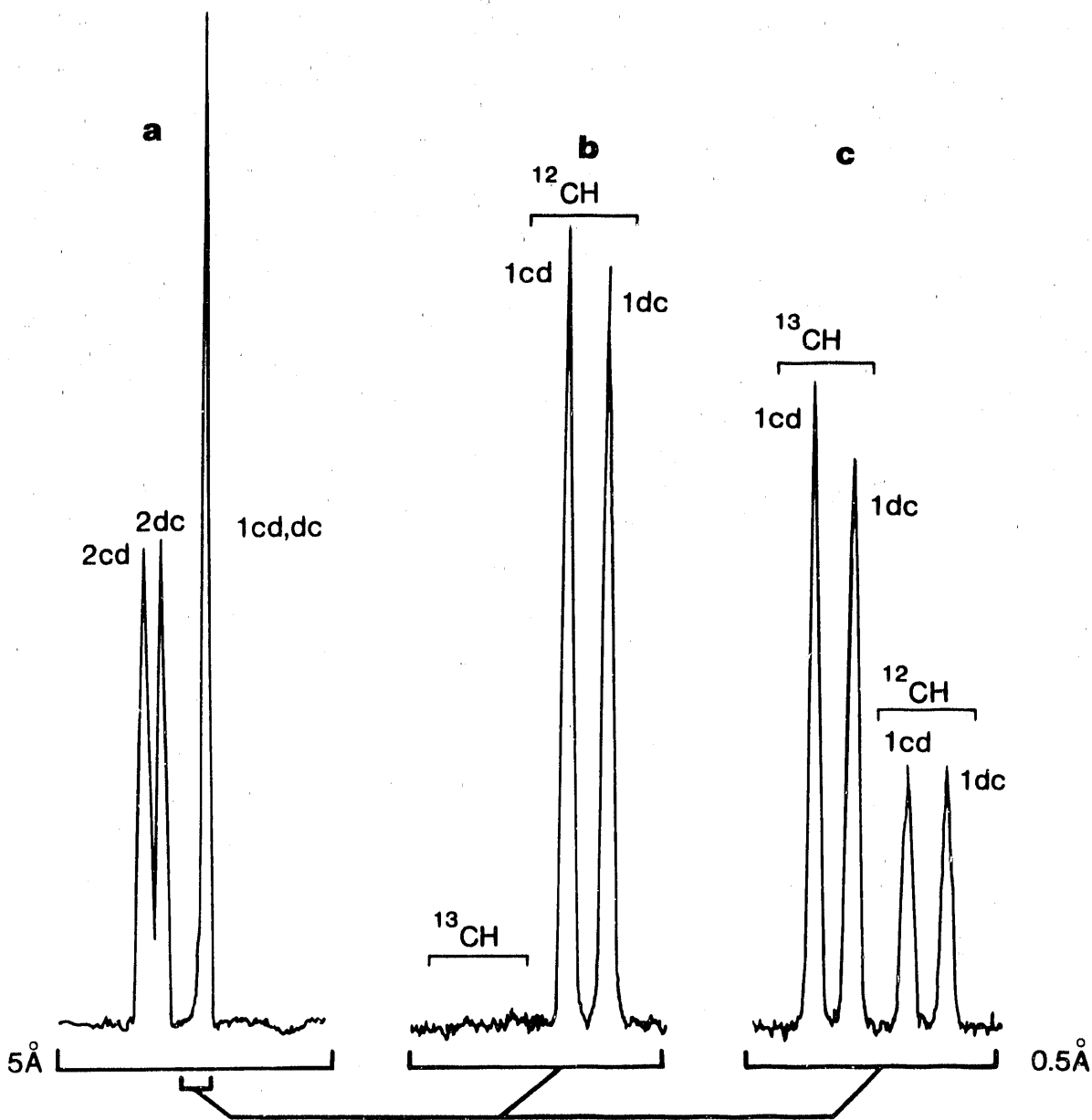


Figure 3. Laser Excitation Spectra in the 0-0 Band of the  $\text{CH}(A+x)$  transition near 432 nm. a) Normal resolution, grating-tuned scan of the F(3) doublets. Wavelength increases to the right. b) High resolution, pressure-tuned etalon scan of the  $\text{P}(3)_1$  component with CH generated from  $^{12}\text{CHBr}_3$ . c) Same as (b), but CH generated from a mixture of  $^{12}\text{C}$  and  $^{13}\text{C}$  bromoform.

P(6)<sub>1dc-1cd</sub> and R(4)<sub>1dc-1cd</sub> splittings (0.68 and 1.45 cm<sup>-1</sup>) and those observed using MODR<sup>15</sup> (0.6618 and 1.451 cm<sup>-1</sup>).

Our results are compared with other work in Table 1 and Figure 4. Note the excellent agreement with the single MODR observation for R<sub>2</sub>(3),<sup>16</sup> and the shift of 0.00 ± 0.03 cm<sup>-1</sup>, for the R(1)<sub>1dc</sub> transition. The curve represents calculated isotope shifts, including electronic, vibrational and rotational contributions, and agrees quite well with our data. The crosses are the data of Richter and Tonner,<sup>17</sup> which clearly do not lie on the calculated curve.

Table 1 - Experimentally Determined Shifts for <sup>13</sup>CH(A ← X) Spectral Lines

Transition	m	Δλ(Å)	Δν (cm <sup>-1</sup> )	Reference
P(6)	-6	-0.252	1.35 ±0.03	This work
P(5)	-5	-0.220	1.18 ±0.03	This work
P(4)	-4	-0.207	1.11 ±0.03	This work
P(3)	-3	-0.162	0.86 ±0.03	This work
R(1)	+2	0.000	0.00 ±0.03	This work
R(2)	+3	+0.036	-0.19 ±0.03	This work
R(3)	+4	+0.059	-0.32 ±0.03	This work
R(3)	+4	+0.059	-0.34 ±0.01	16
R(4)	+5	+0.095	-0.52 ±0.01	This work
R(6)	+7	+0.185	-1.01 ±0.01	17
R(7)	+8	+0.215	-1.18 ±0.01	17
R(8)	+9	+0.248	-1.36 ±0.01	17
R(9)	+10	+0.279	-1.53 ±0.01	17
R(10)	+11	+0.312	-1.73 ±0.01	17
R(11)	+12	+0.345	-1.92 ±0.01	17
R(12)	+13	+0.376	-2.09 ±0.01	17
R(13)	+14	+0.416	-2.32 ±0.01	17
R(14)	+15	+0.449	-2.51 ±0.01	17
R(15)	+16	+0.487	-2.74 ±0.01	17
R(16)	+17	+0.529	-2.98 ±0.01	17

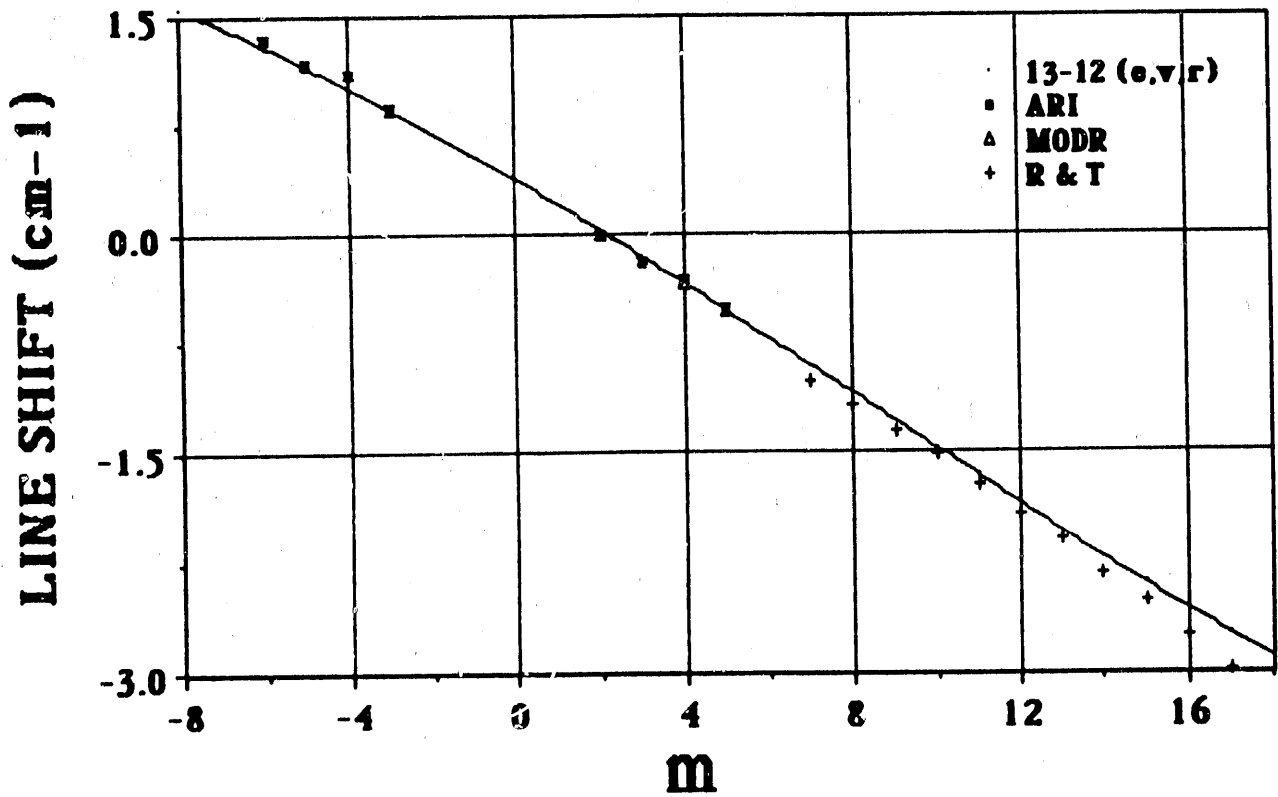


Figure 4. Plot of  $^{13}\text{C}$  Isotopic Shifts for CH. The  $\blacksquare$  represent observations at Aerodyne,  $\blacktriangle$  is the single MODR measurement, and  $+$  are the data of Ref. 17. The curve represents calculated values.

The reason for the discrepancy is not obvious. A simple assignment offset, for example, is ruled out by the unique R(7) multiplet (marked by a near coincidence of the 1cd and 2dc components) which was recorded and assigned as such in Reference 1 and by us. In any case, our measurements should be useful to others studying  $^{13}\text{CH}$  and show that extrapolation of the earlier data to lower J-levels is unreliable. A paper describing these measurements and their interpretation has been prepared for publication.<sup>18</sup>

### 3.3 Kinetic Studies

#### 3.3.1 Overview

Most of the results described here have been published,<sup>13,14</sup> and will only be discussed briefly; manuscripts are included in this report as Appendix A. The subjects of these papers are room temperature studies of the reactions of CH with  $\text{Cl}_2$ ,  $\text{CH}_4$ ,  $\text{N}_2\text{O}$ ,  $\text{O}_2$ ,  $\text{H}_2$ ,  $\text{CO}$  and  $^{13}\text{CO}$ . Preliminary studies of the CH +  $\text{D}_2$ ,  $\text{NO}$ , and  $\text{N}_2$  reactions are also discussed. All kinetic data were obtained and analyzed in the same way, with the exception of those for CH +  $\text{N}_2$  and  $^{13}\text{CO}$ . The experimental procedure, results, and implications for future work are discussed below.

#### 3.3.2 Procedure

Methylidyne concentrations were monitored by laser excited fluorescence, using either the strong  $\text{Q}_1(2)$  or  $\text{R}_1(1)$  doublets, or the  $\text{P}(3)$  multiplet (for  $^{13}\text{C}$  work). The radical source was positioned  $\approx 43$  cm upstream of the detector. Flow speeds were always near  $1000 \text{ cm}\cdot\text{sec}^{-1}$ ; gas flow rates, pressures, and temperatures were monitored with calibrated electronic and rotametric flowmeters, capacitance manometers and both fixed and moveable thermocouples, respectively. Reagents were added through the injector, which was moved between 8 and 38 cm upstream of the detector to effect pseudo-first order decays of  $[\text{CH}]$ .

These were fitted to extract  $k^I$ 's, which were appropriately corrected for transport effects. Typically, the correction factors applied were 1.6-1.7, as expected for diffusion-controlled radical loss at the reactor wall in laminar flow. The correctness of this assumption was demonstrated by observing a doubling of the CH wall loss rate upon halving the total pressure. Plots of corrected  $k^I$ 's against reagent concentration yielded bimolecular rate constants.

This procedure was modified during studies of the CH + N<sub>2</sub> reaction, which proceeds so slowly that massive additions of N<sub>2</sub> through the injector (up to 10% of total reactor flow) were required to observe the decays. The increase in flow velocity at the injector reduced the source-to-detector flow time, and thus the cumulative CH loss as the injector was withdrawn.

Injector traverses with noble gases substituted for N<sub>2</sub> were recorded and used as references for the N<sub>2</sub> decays. Equivalence of total pressure, read with a resolution of 1/2000 at 2 Torr, was used to set the substituent flows. Point-by-point signal ratios were taken to represent the homogeneous process, yielding  $k^I(N_2)$ ; this procedure is summarized in Figure 5. Subsequent data analysis was the same as described above.

For the CH + <sup>13</sup>CO rate constant measurements, the range of injector positions was limited due to the reduced LEF sensitivity (dye laser power) at high resolution. Relative rate measurements for wall-less, mixing-limited conditions were also performed to evaluate the role of wall reactions on the conventional kinetic data. These are described below.



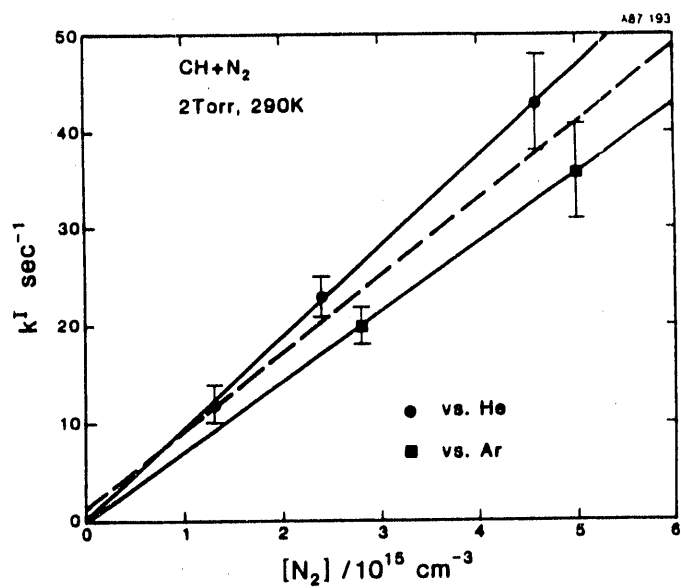
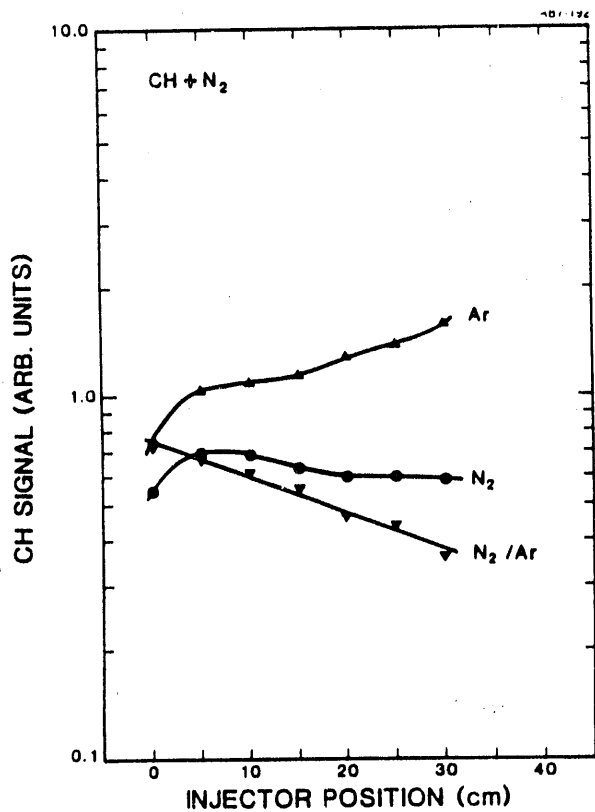


Figure 5. A Typical Decay (left) for CH + N<sub>2</sub>, Showing Injector Traverses with Ar (▲), N<sub>2</sub> (●) and the N<sub>2</sub>/Ar Signal Ratios (▼). Resulting bimolecular plot (right) for CH + N<sub>2</sub>, showing pseudo first-order rates referenced to He (●) and Ar (■).

### 3.3.3 Results and Discussion

A summary of bimolecular rate coefficients measured to date is presented in Table 2. The quoted uncertainties are single standard deviation, and include both random and estimated 15% systematic errors.

Table 2 - Bimolecular Rate Coefficient for CH Reactions at 2 Torr He Near Room Temperature Measured Using the Aerodyne Fast-flow Reactor

REAGENT	RATE COEFFICIENT
	( $\times 10^{-11} \text{ cm}^{-3} - \text{sec}^{-1}$ )
NO	17.0 $\pm$ 4.0
Cl <sub>2</sub>	15.0 $\pm$ 4.0
D <sub>2</sub>	7.7 $\pm$ 2.0
CH <sub>4</sub>	5.4 $\pm$ 1.0
N <sub>2</sub> O	4.2 $\pm$ 0.7
O <sub>2</sub>	2.3 $\pm$ 0.5
<sup>13</sup> CO	0.24 $\pm$ 0.03
H <sub>2</sub>	0.075 $\pm$ 0.012
CO	0.027 $\pm$ 0.003
N <sub>2</sub>	(8.2 $\pm$ 1.5) $\times 10^{-4}$

These results are compared with work from other laboratories in Figure 6, and discussed in turn below. Agreement regarding relative reactivities is very satisfying, spans more than four order of magnitude, and suggests that there are no serious problems with our method. In absolute terms our values tend to be slightly (10-30%) below those previously reported. The reason for this minor discrepancy, which may be resolved by further measurements, is not

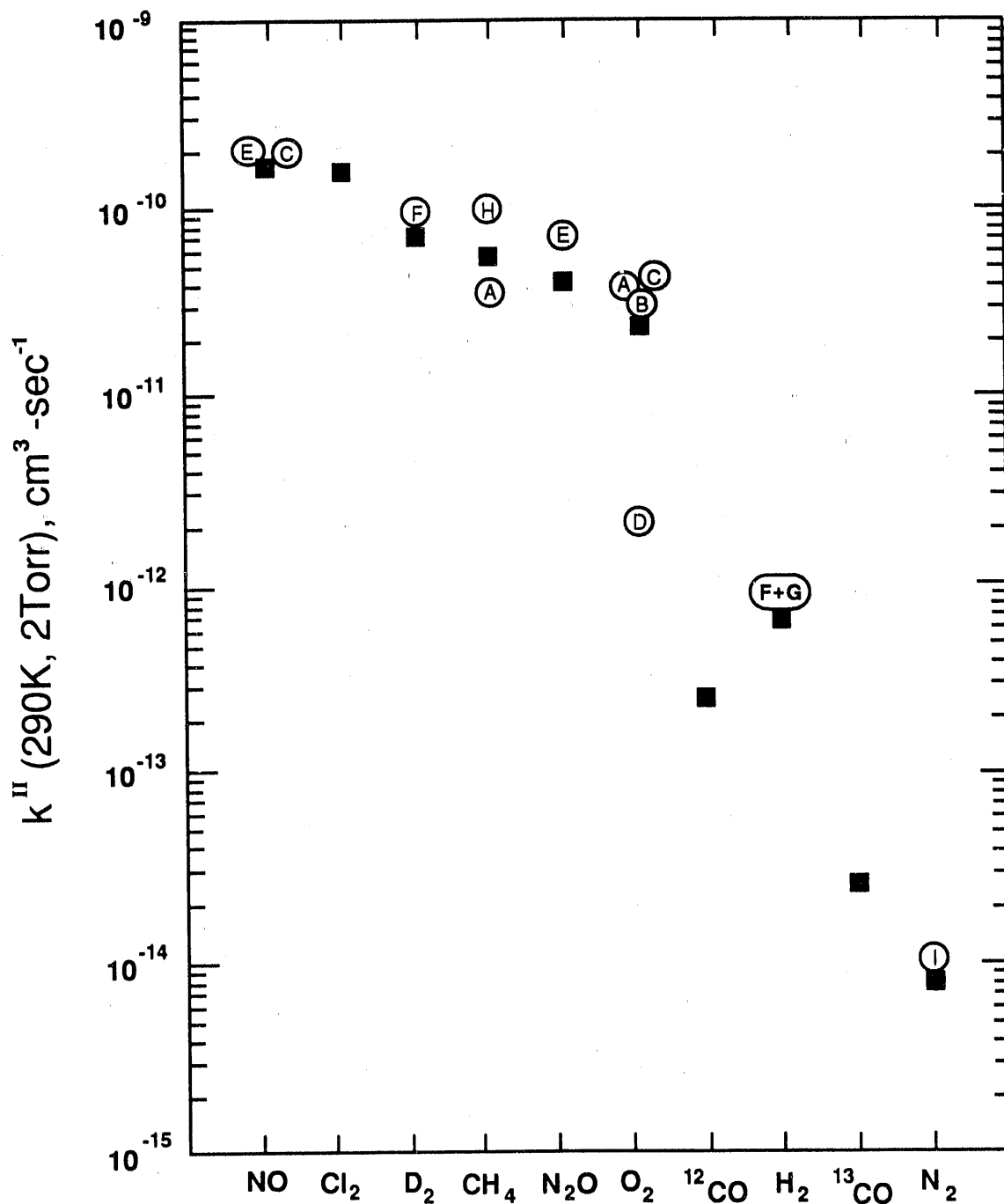


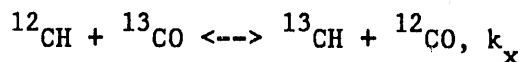
Figure 6. Comparison of Our Results with Those of Other Laboratories. The symbols A-I correspond to data reported in Refs. 19, 8, 10, 20, 9, 6, 21, 22, 4, respectively. F + G means the sum of 2- and 3-body rate constants reported in those papers evaluated for our experimental conditions.

clear but may involve non-thermal internal energy in CH produced in the photolytic sources.

Study of the CH + D<sub>2</sub> reaction was motivated by the additional information it conveys about the H<sub>2</sub> process. It has been examined only once before, and was found to be very fast, with a rate constant of 1.14 x 10<sup>-10</sup> cm<sup>3</sup>-s<sup>-1</sup> at 100 Torr and 297 K.<sup>6</sup> Isotope exchange occurring through the energy-rich CHD<sub>2</sub> intermediate appears to be responsible for 80-85% of this rate, or 9.5 x 10<sup>-11</sup> cm<sup>3</sup>-s<sup>-1</sup>; the rest is due to recombination. Our measurements support this finding, yielding k(D<sub>2</sub>) = (7.7 ± 2.0) x 10<sup>-11</sup> cm<sup>3</sup>-s<sup>-1</sup> at 2 Torr and 290 K.

Brief kinetic studies of CH + NO were undertaken as an additional check against previous work. The data shown in Figure 8 gave a rate constant of (1.7 ± 0.4) x 10<sup>-10</sup> cm<sup>3</sup>-s<sup>-1</sup>, in excellent agreement with other reported values, 1.9 ± 0.3,<sup>4</sup> and 2.0 ± 0.3,<sup>10</sup> in the same units. The most important aspect of this reaction is the nature of the products; our work on this question is described in Section 3.4.

Practical interest in the CH + CO reaction is motivated by its sister process, CH + N<sub>2</sub>. CO is isoelectronic with N<sub>2</sub>, both have 1 $\Sigma^+$  electronic ground states, and consumption of CH by either reagent near room temperature is dominated by 3-body recombination.<sup>4,10</sup> Additional insight into the CH + N<sub>2</sub> mechanism could be obtained by studying the isotope exchange reaction:



This process is also of fundamental interest due to the chemical similarity of CH(X) and CH<sub>2</sub>(<sup>1</sup>A<sub>1</sub>)<sup>23</sup> and the evidence for fast C-exchange in CH<sub>2</sub> + CO.<sup>24</sup> The latter has received considerable theoretical attention.<sup>25-29</sup>

We first estimate the rate coefficient for CH + CO association by fitting a standard fall-off curve to 2-body rate constants for the unlabeled reaction

from our own work at 2 Torr ( $(2.7 \pm 0.3) \times 10^{-10} \text{ cm}^3\text{-sec}^{-1}$ ) and previous measurements at higher pressures. This procedure yielded  $k_{\infty} \approx 1.1 \times 10^{-10} \text{ cm}^3\text{-sec}^{-1}$ , and  $k_0 \approx 4.9 \times 10^{-30} \text{ cm}^6\text{-sec}^{-1}$ . Then, the rate coefficient for C-atom exchange was measured in two ways, both of which employed  $^{13}\text{C}$ -labeled CO and high resolution isotope-selective LEF. Conventional kinetic measurements, which are summarized in Figure 7, gave  $k_x = (2.1 \pm 0.3) \times 10^{-12} \text{ cm}^3\text{-sec}^{-1}$ . In the second method, reagents were added just upstream of the LEF field of view to eliminate wall reactions. Relative rate ratios for consumption of CH by CO, O<sub>2</sub> and  $^{13}\text{CO}$  were identical with those obtained previously; the exchange is indeed homogeneous. Note that  $k_x$  lies about a factor of 50 below the high pressure limit.

Detailed analysis of energy and entropy restrictions suggests that the mechanism involves formation of a quasi-linear HC<sub>2</sub>O complex through a moderately tight transition state, followed by isomerization through a symmetric oxiryl radical to accomplish the exchange. (Note that the previous study of the CH + N<sub>2</sub> process concluded that the transition state leading to HCN<sub>2</sub> was very loose.)<sup>4</sup> Entropy appears to be the controlling factor. Association may occur either by insertion or C-C bond formation; the A-factors estimated using standard methods can accommodate either equally well. Study of the temperature dependence would be valuable in testing the proposed mechanism.

The CH + N<sub>2</sub> reaction is perhaps the most important of all those studied here. Its small rate constant near 300K requires a slightly altered experimental procedure, in which inert gases (Ar, He) were substituted for N<sub>2</sub> to provide unreactive gas baseline profiles of [CH] (see Figure 5). The results suggest that slightly different behavior was obtained for Ar and He, with the N<sub>2</sub> decays referenced to He yielding the larger rate constant. The cause is probably impurities in the UHP Ar substituent.

Extension of the present work to higher temperatures should be straightforward. The precision of the measurements at 290K indicates that

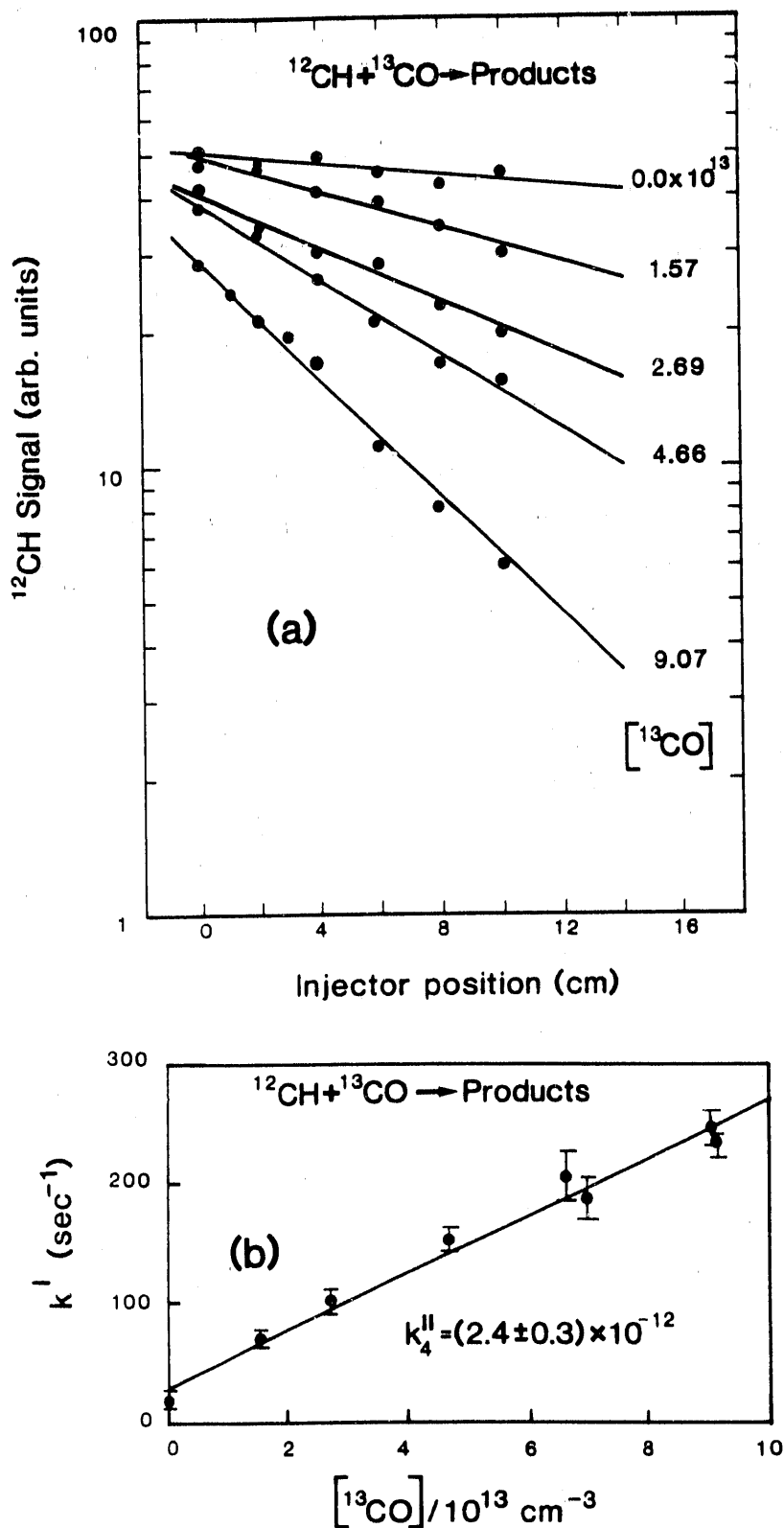


Figure 7. a) Pseudo First-order Decays Observed in the Overall Reaction of  $^{12}\text{CH}$  with  $^{13}\text{CO}$ .  $^{12}\text{CH}$  monitored at  $\text{P}(3)_{1\text{dc}}$  with narrowed laser linewidth. Fitted line in (b) corresponds to  $k_4^{II} = (2.4 \pm 0.3) \times 10^{-12} \text{ cm}^3\text{-sec}^{-1}$ .

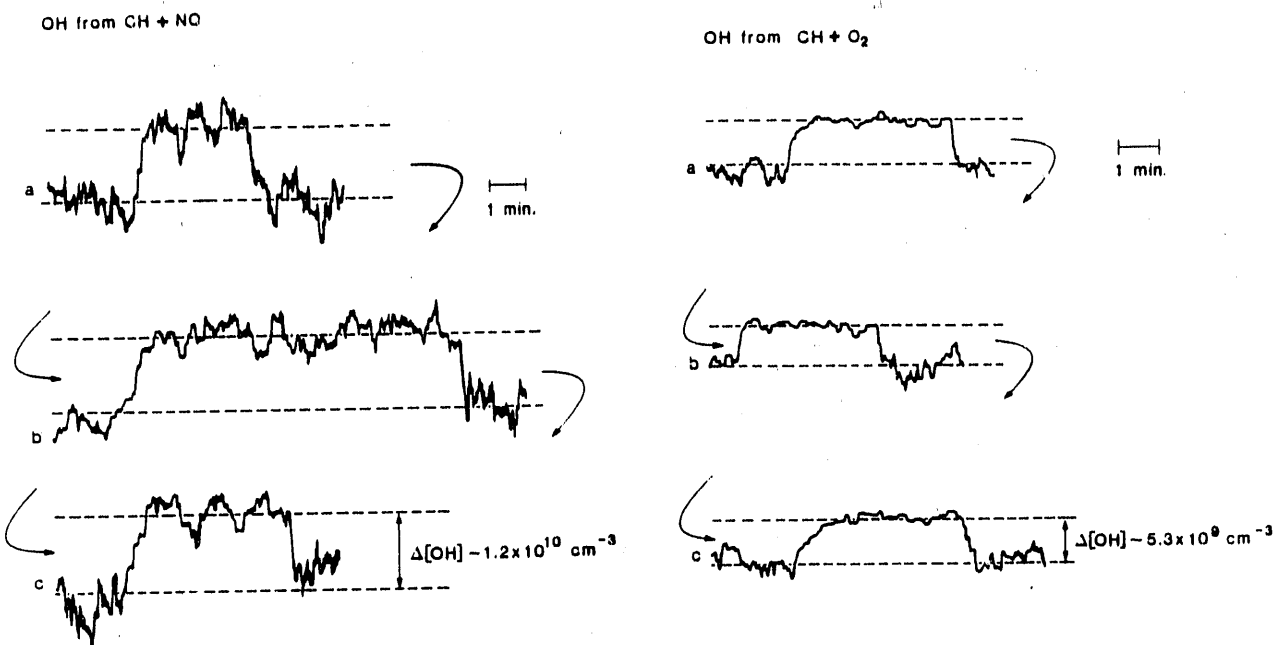


Figure 8. Traces of OH LIF Signals As a Function of Time, During Reaction of CH with NO (left) and O<sub>2</sub> (right). The symbols a-c denote chronologically sequential traces. For CH + NO, [NO] spans an order of magnitude from a (lowest) to c (highest). For CH + O<sub>2</sub>, a-c all used the same [O<sub>2</sub>], sufficient to reduce CH LIF signals by 50%.

decay rates 10-20 times smaller, corresponding to bimolecular rate constants of  $\approx 5 \times 10^{-16} \text{ cm}^3\text{-s}^{-1}$ , can be detected for flow velocities of  $1000 \text{ cm-s}^{-1}$ . Decreased flow speed and increased total pressure will lower this limit and reduce the amount of  $\text{N}_2$  (relative to the total flow) required to produce similar first order rates. This approach will permit greater precision in mapping out the Arrhenius plot.

At the highest temperatures, we expect that increased CH wall loss rates, due to the temperature dependence of the diffusion coefficient, may establish the smallest detectable decay rates. Operation at 10 Torr and 1500K will produce number densities equivalent to 2 Torr and 300K, while wall losses might be expected to double. Increased sensitivity will therefore be required to offset the smaller radical concentrations at the detector. The use of filters in the fluorescence detection optics (required to discriminate against blackbody radiation from the flowtube) should significantly reduce the alkali chemiluminescence which presently sets our detection limit for CH radicals. We should be able to explore the transition between three- and two-body mechanisms occurring near 900K without great difficulty.

### 3.4 Experiments At Elevated Temperatures

Several attempts were made to produce CH with the main reactor operating at 1100K. We could not detect CH using either of the  $\text{CHBr}_3$  or  $\text{CHCl}_3$  precursors, with K-atoms as the abstractor. The problem was traced to thermal decomposition of the CH precursor by operating the main reactor at room temperature and heating the external wall of the source tube. The temperature of the annulus carrying the precursor could thus be altered independently of that in the source or the main flow tube, with the source operating normally. With  $\text{X}=\text{Br}$ , CH signals disappeared when the temperature of the outer tube reached 500K, and reappeared as the tube cooled off. We were unable to duplicate this for  $\text{X}=\text{Cl}$ ; the heating apparatus limited the maximum temperature



to 550K. We fully expect, based on our initial observations, that  $\text{CHCl}_3$  would have dissociated well below 1100K.

Modifications of the radical source to prevent decomposition of the CH precursor were designed and fabricated. This was done without significantly disrupting the temperature of the main reactor gases in the reaction zone by adding a radiatively shielded water jacket to a new source tube.

### 3.5 Product Channel Observations

#### 3.5.1 Overview

The identity of product species, as opposed to reaction rate constants, is of dominant import for several methylidyne reactions, including  $\text{CH} + \text{O}_2$ ,  $\text{NO}$  and  $\text{N}_2\text{O}$ . As discussed previously, there is a profusion of energetically accessible pathways for these reactions, and their impact on the chemical systems in which they occur depends on which are actually taken.

Our approach was to focus on the two simplest reactions first, namely  $\text{CH} + \text{O}_2$  and  $\text{NO}$ , and to attempt quantitative detection of OH. These reagents also suffer the least possible interaction with the alkali atoms;  $\text{NO}$  does not react at all, and  $\text{O}_2$  recombines very slowly. Detection limits for OH, with the CH source off, were  $\approx 10^8 \text{ cm}^{-3}$ ; with the source on, they degraded to  $\approx 10^9 \text{ cm}^{-3}$  due to alkali chemiluminescence.

#### 3.5.2 Procedure

Once the CH source was operating normally, as verified by LEF, it was positioned 15 cm from the detection zone. The dye laser wavelength was changed to excite the  $\text{Q}_1(1)$  line of OH at 307.844 nm. OH signals were calibrated via the  $\text{H} + \text{NO}_2$  reaction, with H from an upstream discharge of  $\text{H}_2/\text{He}$  in large excess. After the calibration, the  $\text{NO}_2$  and  $\text{H}_2$  flows were valved off and the discharge was extinguished, to prevent any chemistry associated with these species. The desired O-containing molecules were then

added either through the injector or another inlet which allowed smaller contact distances. OH signals were recalibrated after these observations were complete.

### 3.5.3 Results and Discussion

Our results are summarized in Figure 8, which presents a time history of the OH signals observed during additions of NO and O<sub>2</sub> as described above. Note that the reagent-off levels correspond within the background noise to [OH]=0. For NO, even the smallest amounts used were sufficient to drive the reaction to completion, while for O<sub>2</sub> only 50% of the CH had been consumed. Subsequent experiments with O<sub>2</sub> in which both the appearance of OH and the disappearance of CH were monitored showed the expected monotonic increase and decrease respectively, but the S/N for OH was insufficient to pin down the temporal relationship with confidence. Source [CHBr<sub>3</sub>]<sub>0</sub> in these experiments was  $\approx 5 \times 10^{11} \text{ cm}^{-3}$ , corresponding to maximum [CH]<sub>0</sub> of  $5 \times 10^{10}$  in the flow tube just downstream of the source outlet.

Although it appears that OH is a major product of both reactions, these observations beg the question of whether or not the OH we have seen is a primary product. It seems fortuitous that both should produce the same amount of OH. For CH + O<sub>2</sub>, large OH yields are not unexpected. For CH + NO, however, experimentally useful concentrations of NH(A) have been observed<sup>30-31</sup> and it may be that considerable ground-state NH is also formed. In the present experiments, this radical could react with NO to form OH, although N<sub>2</sub>O + H are thought to be the preferred product channels.<sup>32</sup>

#### 4.0 CONCLUSIONS

We have come close to satisfying the objectives of this program. Two papers have been published,<sup>13,14</sup> and a third has been submitted for publication.<sup>17</sup> A new CW source of CH radicals suitable for use in fast-flow reactors has been successfully developed and characterized.

Measurements of rate coefficients for ten reactions: CH + NO, Cl<sub>2</sub>, D<sub>2</sub>, CH<sub>4</sub>, N<sub>2</sub>O, O<sub>2</sub>, <sup>13</sup>CO, H<sub>2</sub>, CO and N<sub>2</sub> have been carried out near room temperature in helium at low pressure (2 Torr). Agreement with previous work, where available, is satisfactory. The CH + Cl<sub>2</sub> and <sup>13</sup>CO reactions had not been studied before, nor had the <sup>13</sup>C isotopic line shifts at low J. Observations of C-atom exchange in the CH + CO reaction provided new information on the HC<sub>2</sub>O intermediate, which should be analogous to the HCN<sub>2</sub> intermediate in the CH + N<sub>2</sub> reaction.

A new radical source assembly, incorporating design changes indicated in preliminary high temperature runs, was fabricated, but could not be tested before the end of the grant period. As a result, no high temperature studies were carried out. A search for OH products from the CH + NO and O<sub>2</sub> reactions was initiated. Preliminary data suggest that it is a major product of both reactions at room temperature.

## 5. REFERENCES

1. Sanders, W.A. and Lin, M.C., "Kinetics and Mechanisms of Methylidyne Radical Reactions," in Chemical Kinetics of Small Molecules, Z. Alfassi, ed., CRC Press (in press, 1986).
2. Blauwens, J., Smets, B., and Peeters, J., "Mechanism of "Prompt" NO Formation in Hydrocarbon Flames," 16th Symposium (Int.) on Combustion, p. 1055 (1976); Benson, S.W., Ibid, p. 1062.
3. Glarborg, P., Miller, J.A., and Kee, R.J., "Kinetic Modeling and Sensitivity Analysis of Nitrogen Oxide Formation in Well-Stirred Reactors," Combustion and Flame **65**, 177 (1986).
4. Berman, M.R., and Lin, M.C., "Kinetics and Mechanism of the CH + N<sub>2</sub> Reaction. Temperature and Pressure Dependence Studies and Transition State Theory Analysis," J. Phys. Chem. **87**, 3933 (1983).
5. Butler, J.C., Fleming, J.W., Goss, L.P., and Lin, M.C., "Kinetics of CH Radical Reactions with Selected Molecules at Room Temperature," Chemical Physics **56**, 355 (1981).
6. Berman, M.R. and Lin, M.C., "Kinetics and Mechanisms of the Reactions of CH and CD with H<sub>2</sub> and D<sub>2</sub>," J. Chem. Phys. **81**, 5743 (1984).
7. Dunning, T.H., Jr., Harding, L.B., Bair, R.A., Eades, R.A., and Shepard, R.L., "Theoretical Studies of the Energetics and Mechanisms of Chemical Reactions: Abstraction Reactions," J. Phys. Chem. **90**, 344 (1986).
8. Messing, I., Sadowski, C.M., and Filseth, S.V., Chem. Phys. Lett. **66**, 95 (1979).
9. Wagal, S.S., Carrington, T., Filseth, S.V., and Sadowski, C.M., Chem. Phys. **69**, 61 (1982).
10. Berman, M.R., Fleming, J.W., Harvey, A.B., and Lin, M.C., 19th Symposium (Int.) Combustion, the Combustion Institute, Pittsburgh, PA, p. 73 (1982).
11. Lichtin, D.A., Berman, M.R., and Lin, M.C., "NH (A<sup>3</sup>  $\pi$  + X<sup>3</sup>  $\Sigma^-$ ) Chemiluminescence From the CH (X<sup>2</sup>  $\pi$ ) + NO Reaction," Chem. Phys. Lett. **108**, 18 (1984).

12. Lin, M.C., "The Mechanism of CO Laser Emission From the CH + NO Reaction," J. Phys. Chem. 77, 2726 (1973).
13. Anderson, S.M., Freedman, A., and Kolb, C.E., "Fast Flow Studies of CH Radical Kinetics at 290 K," J. Phys. Chem. 91, 6272 (1987).
14. Anderson, S.M., McCurdy, K., and Kolb, C.E., "The CH + CO Reaction: Rate Coefficient for Carbon Atom Exchange at 294 K," J. Phys. Chem., in press (1988).
15. Brazier, C.R. and Brown, J.M., Can. J. Phys. 62, 1563 (1984).
16. Woodward, D.R., "High Resolution Spectroscopy of Transient Species," D. Phil. Thesis, University of Oxford (1986).
17. Richter, J. and Tonner, K.F., Z. Fur Astrophysik 67, 155 (1967).
18. Anderson, S.M. and McCurdy, K., "J. Mol. Spec.", to be submitted (1989).
19. Bosnali, M.W. and Perner, D., "Reaction von Pulsradiolytisch Erzeugtem CH(<sup>2</sup>Π) mit Methan und anderen Substanzen," Z Naturforsch 26, 1768 (1971).
20. Ducanson, Jr., J.A. and Guillory, W.A., J. Chem. Phys. 78, 4958 (1983).
21. Zabarnick, S., Fleming, J.W., and Lin, M.C., J. Chem. Phys. 85, 4373 (1986).
22. Berman, M.R. and Lin, M.C., Chem. Phys. 82, 435 (1983).
23. James, F.C., Choi, H.K.J., Ruzsicska, B. and Strausz, O.P., "The Gas Phase Chemistry of Carbynes," in Frontiers of Free Radical Chemistry, 1980 ACADEMIC PRESS, INC., pp. 139-69.
24. Montague, D.C. and Rowland, F.S., J. Am. Chem. Soc. 93, 5381 (1971).
25. Dewar, M.J.S. and Ramsden, C.A., "J. Chem. Soc. Commun. 688 (1973).
26. Basch, H., "The Oxirene Intermediate in the Ketene-Methylene + CO System," in Chemical and Biochemical Reactivity, The Jerusalem Symposia on Quantum Chemistry and Biochemistry, VI, Israel Academy of Science and Humanities: Jerusalem, 1974, pp. 183-8.
27. Strausz, O.P., Gosavi, R.K., Denes, A.S. and Csizma a, I.G., J. Am. Chem. Soc. 98, 4784 (1976).

28. Dykstra, C.E., J. Chem. Phys. 68, 4244 (1978).
29. Tanaka, K. and Yoshimine, M., J. Am. Soc. 103, 7655 (1980).
30. Nishiyama, N., Sekiya, H., Yamaguchi, S., Tsuji, M., and Nishimura, Y., "Internal Energy State Distribution of  $\text{NH}(\text{A}^3\pi, v''=0)$  From the Chemiluminescent Reaction of  $\text{CH}(\text{X}^2\pi, v''=0)$  with  $\text{NO}$ ," J. Phys. Chem. 90, 1491 (1986).
31. Nishiyama, N., Sekiya, H., Tsuji, M., and Nishimura, Y., "Internal Energy Disposal in the Chemiluminescent Reaction  $\text{CD} + \text{NO} \rightarrow \text{NO}(\text{A}) + \text{CD}$  and the Kinetic Isotope Effect," Chem. Phys. 112, 265 (1987).
32. Melius, C.F. and Binkley, J.S., "Energetics of the Reaction Pathways for  $\text{NH}_2 + \text{NO}$  Products and  $\text{NH} + \text{NO}$  Products," 20th Symp. (Int). Combustion, The Combustion Institute, p. 575 (1984).

APPENDIX A

I. FAST FLOW STUDIES OF CH RADICAL KINETICS AT 290 K

II. THE CH + CO REACTION: RATE COEFFICIENT FOR CARBON ATOM  
EXCHANGE AT 294 K

**END**

**DATE  
FILMED**

*2 / 25 / 92*



